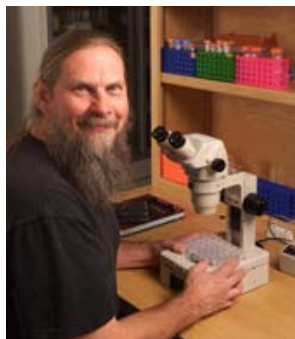




NE-CAT Communications

A Biannual Newsletter of the Northeastern Collaborative Access Team Winter 2013



Message from the Director

Steve Ealick

Welcome to the latest edition of NE-CAT Communications, NE-CAT's biannual newsletter.

In the last newsletter, I stated that we had received funding for our latest NIH grant proposal. In this newsletter, we will share with you some of the ideas and directions presented in the grant. We will also share the progress we already have made in achieving some of the goals we have set for the next five years.

NE-CAT has plans to improve our research capability in the areas of low resolution diffraction and refinement, microbeam technology and new computational algorithms and data management tools to enable optimal and efficient data collection. In each area of interest, NE-CAT has multiple projects in progress. I am very excited about the direction NE-CAT is moving and I hope, after reading this newsletter, that you are too.

For further information on our beamline capabilities or to check out available beamtime, please visit our website at <http://necat.chem.cornell.edu>.

Beamline Developments

1. HC1 Humidity Control Device

Often some projects get stuck at a low resolution diffraction in spite of intense efforts to improve the crystals. Sometimes crystals can be improved by dehydrating them. Crystal dehydration has been documented to affect the packing of the crystal lattice, change the unit cell dimensions, decrease mosaicity, change the space group and increase the diffraction limit. During our low resolution workshop in 2011, we invited a speaker from EMBL-Grenoble to present a

new device capable of regulating the relative humidity (RH) of macromolecular crystals, the HC1. The device has since been commercialized by Maatel and NE-CAT has purchased one. Our HC1 arrived in January 2014.

One important point to remember is that all controlled RH experiments will need to be performed at ambient temperature. When in use, the HC1 takes the place of the cryostream nozzle. It can deliver a smooth stream of air of given humidity onto the sample. This will allow for controlled dehydration of the crystal at the beamline. Diffraction images can be taken at different RH values. If an improved diffraction resolution is found at a particular RH, a number of crystals can be cryo-cooled at that RH and later used for data collection under cryogenic conditions. NE-CAT is in the process of designing a means of smoothly transitioning between the HC1 and the cryostream nozzle. This will reduce the time required to change out the cryostream head.

The HC1 is comprised of a machine body with a humidity nozzle that points the humid airstream onto the sample and a PC with software that allows control of the different parameters (Fig. 1). The machine body holds the dew point generator/controller, air flow meters, peristaltic pumps, hot water bottle and a water reservoir. Using the dew point to keep the relative humidity independent of temperature, the humid airstream is generated by removing water from a hot



Fig. 1 The HC1 sitting inside the 24-ID-E hutch. The machine body is in the foreground and the cart holding the PC is in the background.

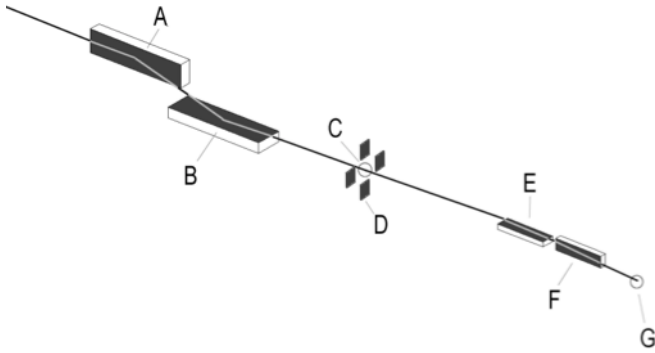


Fig. 2 Schematic of 24-ID-E secondary Kirkpatrick Baez focusing system. A: primary horizontal focusing mirror; B: primary vertical focusing mirror; C: Slits; D: Primary focus, E: Secondary vertical focusing mirror; F: secondary horizontal focusing mirror; G: secondary focus point (MD2 spindle). Note: the order of the vertical and horizontal components of the primary and secondary KB systems is reversed to improve focus spot symmetry of the secondary focus.

and moisture-saturated airstream. It is then channeled to the sample whereupon it reaches the user-selected RH.

You may visit the NE-CAT website to see the video of the presentation on the HC1 (<http://necat.chem.cornell.edu/workshops/lowresolutionworkshop.php>).

2. Beamline 24-ID-E Optics Upgrade

In the Winter 2010 newsletter, we presented a potential redesign of the fixed-energy 24-ID-E beam line optics to provide a significantly higher flux and brilliance by adding a secondary focus using a compound refractive lens (CRL). Since then, the redesign has changed significantly and moved away from use of a CRL. Instead, we have chosen to install a secondary Kirkpatrick-Baez (KB) focusing system upstream of the 24-ID-E MD2 microdiffractometer. Fig. 2 is a schematic of the revised 24-ID-E focusing optics.

The existing single focus KB system currently provides a focus spot at the MD2 spindle axis of 15×100 microns (3σ) with a total intensity of $\sim 1 \times 10^{13}$ photons / sec at 12.662 KeV. Our goal is to generate a focus spot of $\sim 8 \times \sim 10$ micron (V x H) and increase the flux when using the smallest aperture (currently 5 μm) by 1 to 2 orders of magnitude.

Using funds from a Keck Foundation grant to David Eisenberg of UCLA and NE-CAT institutional funding,

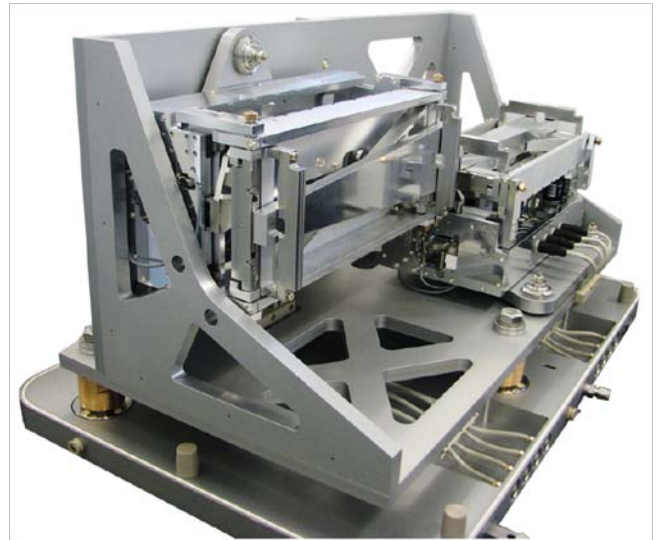


Fig. 3 Photograph of the compact KB focusing system with the vacuum vessel removed as viewed from downstream. This system is based on designs by P. Ing (Physics, U. Chicago, CARS – APS).

NE-CAT ordered a compact KB focusing system (Fig. 3) from Instrument Design Technology (Widnes, UK) consisting of a support and bending mechanisms for 2 trapezoidal, rhodium-coated silicon mirror flats (320 mm length) and a UHV vacuum chamber. The support structure includes bending and precision positioning mechanisms for both mirrors. Both horizontal and vertical mirrors were assayed by the APS metrology group in August 2013 and yielded excellent metrological properties with surface roughness less than 1 Å r.m.s. and slope errors less than 0.5 microradians.

The mirror system and vacuum vessel will require a new support structure that must be designed and built. The current plan is for the extensible collimator assembly to be removed from its location upstream of the A-frame holding the detector. The various subsystems connected to the current collimator assembly (monochromatic beam position monitor, attenuator array, data collection shutter) will be moved to supports attached to the new compact KB vacuum vessel.

A four-blade motorized slit assembly will be installed at the secondary source point (Fig. 2, label C). We will be able to operate the compact, secondary KB system in a number of different modes: 1) re-imaging of the secondary source to a focus at the MD2 spindle; 2) vertical focus provided solely by the compact KB vertical focusing mirror (by dropping the primary vertical focusing mirror out of the beam). In this configuration the vertical focus spot will be reduced to 2 microns, but with some loss in efficiency of capturing the unfocused beam due to the modest length of the secondary vertical focusing mirror compared to the primary VFM.

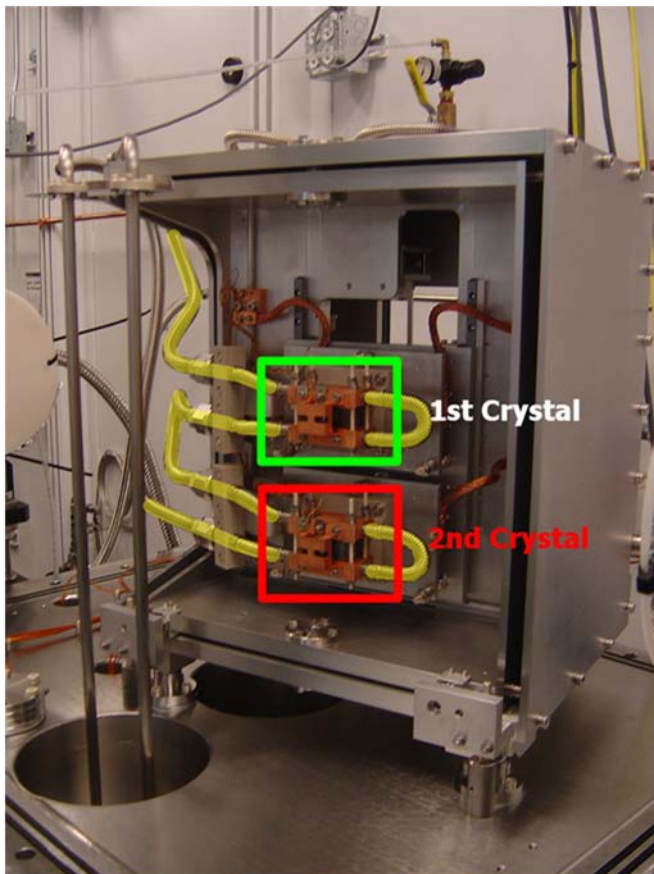


Fig. 4 The current two crystal monochromator on 24-ID-E. The first crystal (green) is the Si 220 cut (12.662 KeV) and the second crystal (red) is the Si 311 cut (14.7 KeV). Highlighted in yellow is the common LN₂ cooling loop.

The 24-ID-E monochromator suffers from beam position instability due to its cooling system. The monochromator crystals are cooled indirectly by two copper blocks, incorporating a liquid nitrogen cooling loop, clamped to the vertical faces (non-diffracting) of the crystals. Two crystals are mounted in the monochromator providing either 12.662 (Si 220 cut) or

14.7 (Si 311 cut) KeV monochromatic radiation at a fixed takeoff angle (Fig. 4). Both crystals are mounted from kinematic mounting modules providing independent pitch, yaw and roll of both crystals. A common liquid nitrogen (LN₂) circulation loop feeds the cooling blocks of both crystal modules. Similar to the hoses on the 24-ID-C monochromator prior to their replacement, these hoses are corrugated and turbulence from LN₂ flow over the corrugation transfers to the crystal modules, resulting in horizontal motion of the focused beam on the order of 1-3 microns r.m.s. This will be unacceptably large for the beam generated by the secondary KB focusing system, causing an estimated 8-10 microns horizontal deviation.

We plan to contract with the original vendor of the 24-ID-E monochromator FMB-Oxford (previously Oxford-Danfysik) to design and manufacture a single, directly-cooled 220-cut Si crystal to replace the existing 2-crystal monochromator configuration. The revised crystal and mount will be more massive, mechanically simpler and more rigid than the current system. This new crystal and mount will be less sensitive to motion from the LN₂ distribution system. In addition, the existing corrugated LN₂ hoses will be replaced with smooth bore tubing with two, short flexible sections for connecting to the new crystal, eliminating flow-induced vibrations.

These changes will also result in converting the 24-ID-E monochromator from indirect to direct LN₂ cooling. This will permit stable operation at 12.662 KeV, using the third harmonic mode of the undulator. Use of the third harmonic increases the power load on the monochromator crystal by more than an order of magnitude, compared to operation using the first harmonic, but will increase the flux at 12.662 KeV by a factor of 2.5-3. The existing monochromator cooling system simply cannot mitigate the power loads incurred with third harmonic operation.

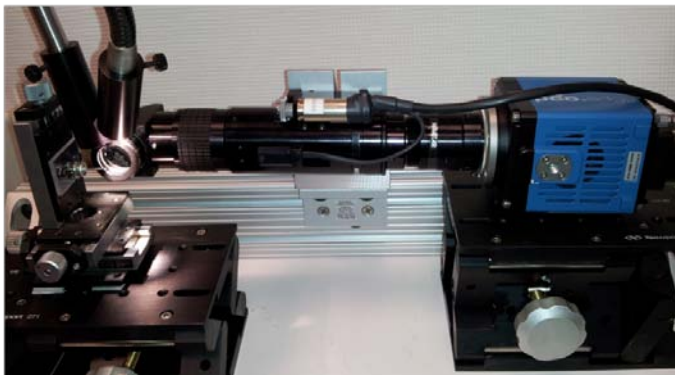


Fig. 5 A) sCMOS Camera in December 2013. B) sCMOS camera refitted with water cooling of its Peltier.

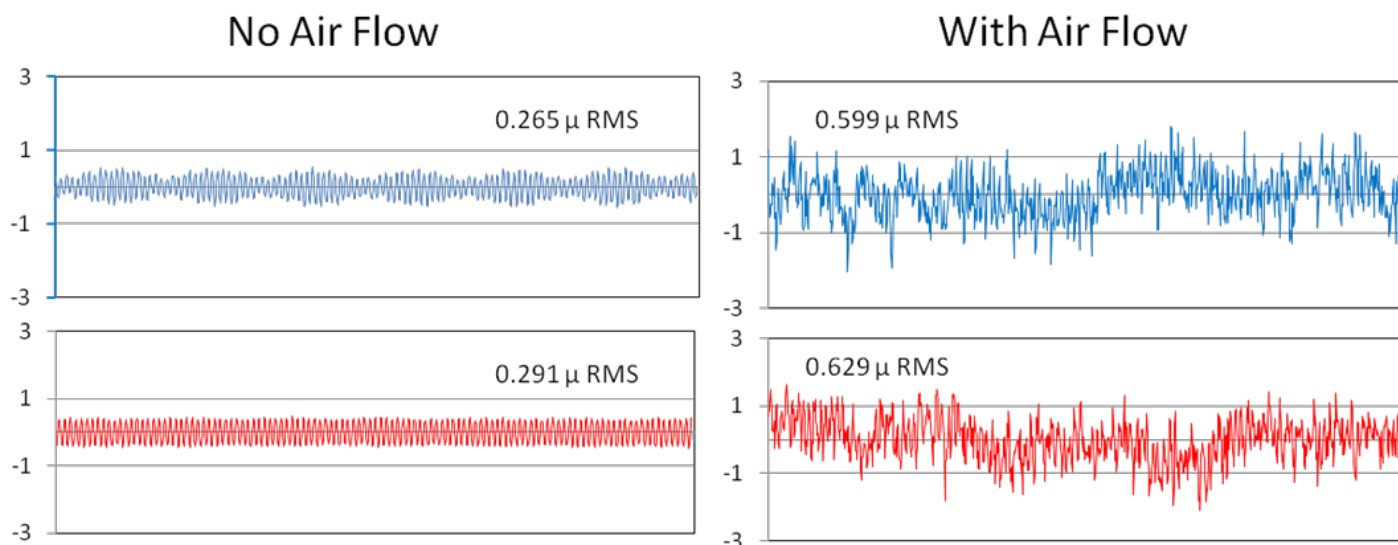


Fig 6. In this experiment, the x and y displacements of an object within the recording field of the camera were measured in the presence and absence of air flow at a frame rate of 1 KHz and an exposure time of 1 msec. The air flow was generated by spraying compressed air gently over the object. The blue line is the displacement of the object along the x-axis. The red line is the displacement of the object along the y-axis.

3. Scientific CMOS Camera

A stable sample is as important as a stable beam. This becomes critical when both samples and beams are micron-sized. Air flow from cryogenic coldstreams is known to cause perturbations in the location of the sample. However, no quantitative measurements have been done so far to our knowledge. NE-CAT plans to obtain real-time aerodynamic stability of sample mounts and beam position via high speed, high resolution videography. These measurements will provide engineering data for design and testing of more stable loops as well as cryostream optimizations, including flow orientation and flow rates.

The first step in obtaining these real-time measurements is the purchase of a scientific CMOS (sCMOS) camera from PCO to replace the CCD camera in the MD2 microdiffractometer (Fig. 5A). The sCMOS camera is capable of rolling shutter readout modes, making it suitable for advance microscopy imaging and scanning such as: lightsheet microscopy, selective plane imaging microscopy (SPIM), structured illumination microscopy, localizations microscopy (GSD, PALM, STORM, dSTORM), or spinning disk confocal microscopy. The ability of the sCMOS to handle these techniques means it has low readout noise, high dynamic range, high resolution, high quantum efficiency and high speed.

The sCMOS camera features temperature-stabilized Peltier cooling of the sensor, allowing for continuous

operation free of drift during image capture. The sCMOS camera was tested in December 2013 and we noticed a periodic disturbance of a test object along the horizontal (Fig. 6). After communicating with PCO, it was discovered that this periodic disturbance is also seen by people in the microscopy community and it is the result of using a fan to cool the Peltier. The solution for the microscopy community was to refit the Peltier device for water cooling. Therefore, we sent the sCMOS camera back to PCO and had the Peltier converted from air cooling to water cooling (Fig. 5B).

4. Resource Advisory Committee Meeting

On January 23, NE-CAT had our first meeting with our new Resource Advisory Committee for the “NE-CAT Center for Macromolecular Crystallography.” As per the P41 guidelines, the Advisory Committee advises on the “future directions for the Center, particularly in planning additional grant applications and in setting priorities for allocation of Center facilities.” The members of our new committee are: Dr. Christopher Hill (Chair, University of Utah), Dr. John Chrzas (SER-CAT, Advanced Photon Source), Dr. Leemor Joshua-Tor (Cold Spring Harbor Laboratory), Dr. Daniel Leahy (Johns Hopkins University School of Medicine), Dr. Corie Ralston (Berkeley Center for Structural Biology, Advanced Light Source), Dr. Douglas Rees (California Institute of Technology), and Dr. Thomas Terwilliger (Los Alamos National Laboratory).

Attending the meeting were Chris Hill, John Chrzas, Daniel Leahy, Corie Ralston, and Doug Rees. Leemor Joshua-Tor participated remotely via WebEx and



Fig. 7 Members of the Advisory Committee in the 24-ID-E hutch. Pictured from left to right are Malcolm Capel, Douglas Rees*, Daniel Leahy*, Corie Ralston*, Christopher Hill*, John Chrzas*, and Steve Harrison. Committee members have an asterisk (*) after their name.

Steve Harrison represented the NE-CAT Executive Committee. Steve Ealick gave an overview and history of NE-CAT, staff presented short talks about our three core Technology, Research and Development (TR&D) areas, and the Advisory Committee provided insight, especially with regards to our Low Resolution Crystallography TR&D given the advances in EM over the last year.

Research Highlights

Mechanisms of non-coding RNA function: co-crystal structure of a T-box riboswitch in complex with tRNA

Adrian R. Ferré-D'Amaré,
Senior Investigator, Laboratory
of RNA Biophysics and Cellular
Physiology
National Heart, Lung and Blood
Institute, NIH, Bethesda, MD



Riboswitches are gene-regulatory domains of mRNAs that directly sense the intracellular concentration of their cognate ligands and modulate transcription, translation or splicing in *cis* (reviewed in Zhang *et al.*, *Biochemistry* **49**:9123, 2010). The T-box, the first riboswitch to be discovered (Grundy & Henkin, *Cell* **74**:475, 1993), is widely used by Gram-positive bacteria (including pathogens such as *Clostridium*, *Listeria*, *Staphylococcus* and *Streptococcus*) to sense amino acid levels and activate expression of genes

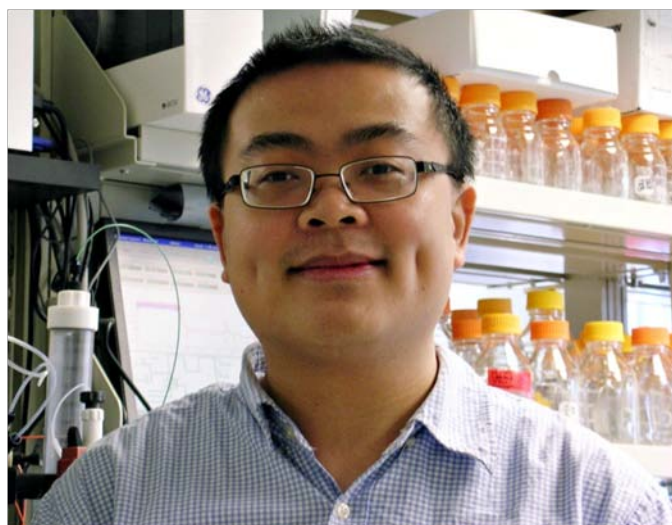


Fig. 8 Jinwei Zhang, Post-doctoral Fellow, who performed the work.

encoding aminoacyl-tRNA synthetases, amino acid transporters, etc., in response to starvation. T-boxes achieve specificity for a particular amino acid employing tRNA as the signaling molecule. These riboswitches decode the anticodon of their cognate tRNA and also sense its aminoacylation status. If the tRNA is not aminoacylated (charged), this is interpreted as starvation.

In the twenty years since their discovery, T-boxes have been subjected to numerous genetic studies. However, how this non-coding RNA achieves specific, high-affinity binding to tRNA remained mysterious. The reason for this became clear when Jinwei Zhang (Fig. 8) joined the Ferré-D'Amaré laboratory and set out to characterize the T-box: *in vitro*, this RNA is conformationally heterogeneous, aggregated, and unsuitable for biophysics. We subjected many T-boxes to deletion, SAXS and calorimetric analyses, ultimately succeeding in generating several candidate RNA constructs that form tight ($K_d \sim 100$ nM), monodisperse complexes with tRNA. This set the stage for crystallographic analysis.

24-ID-C and 24-ID-E are key to success

Promising crystals of a T-box in complex with tRNA were forthcoming after several years of work. As grown, our best co-crystals diffracted synchrotron X-rays only to 8 Å resolution. Their diffraction limit could be dramatically extended (to nearly 3 Å) through a new post-crystallization treatment scheme in which controlled dehydration was combined with exchange of cations needed for crystal growth (Li^+ and Mg^{2+} in this case) with cations with a more flexible coordination geometry (Sr^{2+}). The improvement in resolution, however, did not suppress a tendency for these plate-shaped orthorhombic crystals to crack and produce

poor diffraction spot profiles. Additional difficulties in data collection were the pronounced radiation sensitivity of our crystals, high mosaicity (up to 2°), and a relatively long *c* unit cell edge (*a* ~ 100 Å, *b* ~ 110 Å, *c* ~ 270 Å). After experimenting with several synchrotron beamlines across the country, we obtained the data that allowed us to solve the structure at 24-ID-C and 24-ID-E. Possibly thanks to the beam steering implemented at this facility, we could achieve excellent order-to-order separation, and vector and spiral data collection strategies enabled us to mitigate radiation damage. The occluded view centering available at NE-CAT was very useful because, in order to avoid overlap, we mounted our crystals on loops bent 90° to position the long unit cell edge (and short physical dimension) of the crystals parallel to the rotation axis. Even data with good merging statistics proved to suffer from the effects of incipient radiation damage. Success in MR-SAD phasing only came through systematic merging of multiple datasets, for which we received unstinting help from Drs. Perry and Rajashankar of NE-CAT.

The T-box-tRNA interface is extensive

Our co-crystal structure (Zhang & Ferré-D'Amaré, *Nature* **500**:363, 2013) reveals that the T-box Stem I domain (which we had shown is necessary and sufficient for high affinity binding) folds as an irregular C-shaped helix that cradles the L-shaped tRNA (Fig. 9). Rather than just base-pairing with the tRNA anticodon, the T-box makes an extensive intermolecular interface. Two sets of intermolecular RNA-RNA interactions are noteworthy. First, the three Watson-Crick base pairs made between the anticodon of the tRNA and the "specifier" sequence of the T-box are buttressed by conserved purine bases that stack above and below. This is reminiscent of how the mRNA-tRNA interaction is stabilized in the decoding center of the ribosome. Second, two interdigitated loops near the distal end of the T-box present a flat surface for stacking with the exposed tertiary base pair that is an universal characteristic of the "elbow" of tRNAs. Thus, sequence and structure specificity for tRNA arises from anticodon decoding and shape complementarity, respectively. An unexpected discovery stemming from our structure was that a structural element identical to the interdigitated apical loops of the T-box is also used to recognize the elbow of tRNAs in two completely unrelated contexts: the RNA processing ribozyme RNase P, and the E-site L1 stalk of the bacterial ribosome. Thus, it appears that this strategy for tRNA binding has evolved independently at least three times.

Comparison of our co-crystal structure with structures of tRNA in isolation and fragments of the T-box indicate that the two molecules interact optimally by undergoing mutually induced fit. Binding to the T-box

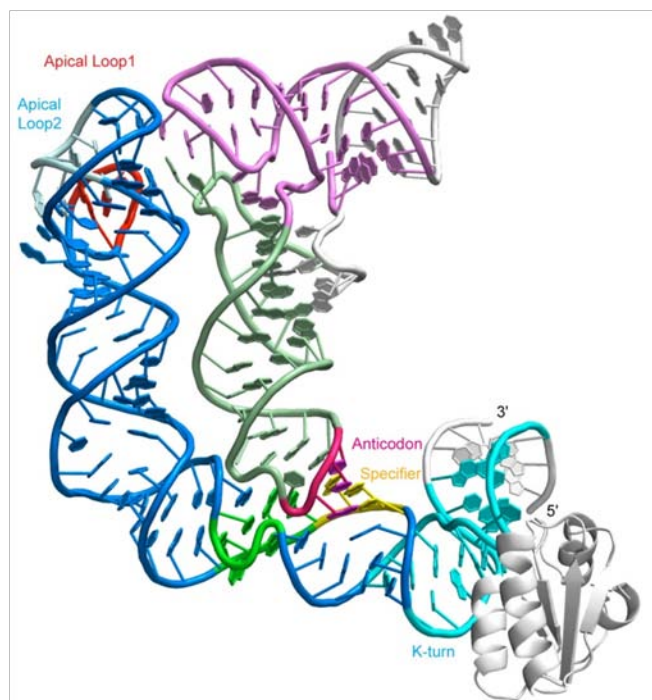


Fig. 9 T-box-tRNA structure. Anticodon from the tRNA is colored magenta. "Specifier" sequence from the T-box is colored yellow. K-turn is colored aqua.

induces a 20° bend in tRNA at a hinge located near the interface of the anticodon and D stems. Structural studies of the ribosome by several groups have previously shown that, as it transits through the ribosome, tRNA bends precisely at the same position. Thus, the T-box exploits intrinsic flexibility of tRNA. The proximal end of the Stem I domain of the T-box contains a conserved K-turn. This structural motif (Klein *et al.*, *EMBO J*, **20**:4214, 2001) introduces a 120° kink in the path of the backbone. In the absence of tRNA, the K-turn of the T-box is not folded (Wang & Nikonowicz, *J. Mol. Biol.*, **408**:99, 2011). Folding of the K-turn induced by tRNA binding is potentially important for T-box function because it directs the 3' element of the riboswitch in the direction of the acceptor terminus of tRNA, with which it needs to interact.

Our co-crystal structure explains how the conserved structural modules of the T-box riboswitch are used to recognize tRNA, and reveals that sequence, molecular plasticity and even post-transcriptional modifications of tRNA are exploited by this non-coding RNA to achieve specificity. Large non-coding RNAs that play critical roles in cells are being discovered at an accelerating pace. Our structure provides general insights into the functional association of two large RNA molecules.

Staff Activities

Meet Our Scientists

Many of our staff members have been with NE-CAT for a long time, making for a stable organization. Besides the four administrative and technical staff members featured in the Summer 2013 newsletter, we have three scientific staff members who have been with NE-CAT over 10 years.



developments, construction, upgrades, and maintenance.

Malcolm Capel joined NE-CAT in 2001, when the 8-BM beamline was transferred from the Whitehead Institute to NE-CAT. He is currently the Deputy Director, responsible for all the day-to-day activities at the beamlines. He also manages the technical staff and is responsible for all technical



performs user support and training for all beam line operation systems, software, detector and hardware. Igor also assists users with optimization of data collection strategies and helps with difficult data processing and structure solution on site. He participates in NE-CAT technological R&D and in commissioning of software and new hardware for NE-CAT beamlines. Igor has several collaborative scientific researches with beamline users, including St. Jude's Children's Research Hospital, the Hormel Institute at the University of Minnesota, Lunenfeld-Tanenbaum Research Institute of Mount Sinai Hospital, Columbia University, and Weill Cornell Medical College.

Igor Kourinov received his PhD from the Institute of Chemical Physics in Moscow. After a postdoctoral fellowship at Thomas Jefferson University in Philadelphia, he worked as a Staff Scientist at AlexanderParker Pharmaceuticals for 5 years prior to joining NE-CAT in November 2002. At NE-CAT, Igor



interest are vitamin B12 binding proteins, flavoenzymes and metallo-proteins. He has 36 peer-reviewed publications in leading journals. He has presented several invited talks at national/international conferences and institutions. At NE-CAT, Sukumar is responsible for supporting and conducting research activities at the beamlines, which includes training of the users in data collection techniques/crystallographic aspects. He is the Safety Coordinator for NE-CAT and is responsible for implementing the APS approved safety (ES&H) plan. He interacts with the APS safety management, and advises the NE-CAT management, staff and users on safety issues. He is responsible for assessing the safety of user experiments, by analyzing their safety training and a sample's biohazard safety level, *ie.* ESAF approval. He is also the Chemical Safety Captain and ascertains NE-CAT's proper use of the ANL Chemical Management System. He also tracks all the hazardous materials at NE-CAT to report to APS on monthly basis.

Narayanasami Sukumar will complete his 11th year at NECAT in February 2014. Sukumar earned his Ph.D in Crystallography and Biophysics from University of Madras, India. Prior to joining NE-CAT, he was a postdoctoral researcher at Washington University, St. Louis. His research areas of

Presentations

Kanagalaghatta Rajashankar, "Dose-sliced Data Collection," 11th International Conference on Biology and Synchrotron Radiation (BSR), Hamburg, Germany, September 8-11, 2013.

Publications

Demirci, H., Wang, L., **Murphy, F. V. t.**, Murphy, E. L., Carr, J. F., Blanchard, S. C., Jogl, G., Dahlberg, A. E., and Gregory, S. T. (2013) The central role of protein S12 in organizing the structure of the decoding site of the ribosome, *RNA* 19, 1791-1801.

Marcia, M., Humphris-Narayanan, E., Keating, K. S., Somarowthu, S., **Rajashankar, K.**, and Pyle, A. M. (2013) Solving nucleic acid structures by molecular replacement: examples from group II intron studies, *Acta Crystallogr. D* 69, 2174-2185.

Lee, K., Gu, S., Jin, L., Le, T. T. N., Cheng, L. W., Strotmeier, J., Krueel, A. M., Yao, G., **Perry, K.**, Rummel, A., and Jin, R. (2013) Structure of a Bimodular Botulinum Neurotoxin Complex Provides Insights into Its Oral Toxicity, *PLoS Pathog.* 9, e1003690.

Windsor, M. A., Valk, P. L., Xu, S., **Banerjee, S.**, and Marnett, L. J. (2013) Exploring the molecular determinants of substrate-selective inhibition of cyclooxygenase-2 by lumiracoxib, *Bioorg. Med. Chem. Lett.* 23, 5860–5864.

Shanmugam, G., Minko, I. G., **Banerjee, S.**, Christov, P. P., Kozekov, I. D., Rizzo, C. J., Lloyd, R. S., Egli, M., and Stone, M. P. (2013) Ring-Opening of the γ -OH-PdG Adduct Promotes Error-Free Bypass by the *Sulfolobus solfataricus* DNA Polymerase Dpo4, *Chem. Res. Toxicol.* 26, 1348-1360.

Kamadurai, H. B., Qiu, Y., Deng, A., Harrison, J. S., Macdonald, C., Actis, M., Rodrigues, P., Miller, D. J., Souphron, J., Lewis, S. M., **Kurinov, I.**, Fujii, N., Hammel, M., Piper, R., Kuhlman, B., and Schulman, B. A. (2013) Mechanism of ubiquitin ligation and lysine prioritization by a HECT E3, *Elife* 2, e00828.

Chen, Y., **Rajashankar, K. R.**, Yang, Y., Agnihothram, S. S., Liu, C., Lin, Y. L., Baric, R. S., and Li, F. (2013) Crystal structure of the receptor-binding domain from newly emerged Middle East respiratory syndrome coronavirus, *J. Virol.* 87, 10777-10783.

Xu, K., Xu, Y., **Rajashankar, K. R.**, Robev, D., and Nikolov, Dimitar B. (2013) Crystal Structures of Lgr4 and Its Complex with R-Spondin1, *Structure* 21, 1683–1689.

Rutherford, K., Yuan, P., **Perry, K.**, Sharp, R., and Van Dyne, G. D. (2013) Attachment site recognition and regulation of directionality by the serine integrases, *Nucleic Acids Res.* 41, 8341-8356.

Committee Participation

Malcolm Capel, ABBIX Final Design Review, Upton, New York, November 10-11, 2013.

Acknowledgements

NE-CAT is supported by a grant from the National Institute of General Medical Sciences (2P41GM103403-11) and contributions from the following NE-CAT institutional members:

Columbia University
Cornell University
Harvard University
Massachusetts Institute of Technology
Memorial Sloan-Kettering Cancer Center
Rockefeller University
Yale University